

# Computer-aided laccase engineering: toward biological oxidation of arylamines

Gerard Santiago<sup>†‡</sup>, Felipe de Salas<sup>§‡</sup>, M. Fátima Lucas<sup>†||‡</sup>, Emanuele Monza<sup>†</sup>, Sandra Acebes<sup>†</sup>, Ángel T. Martínez<sup>§</sup>, Susana Camarero<sup>§\*</sup>, Víctor Guallar<sup>†¥\*</sup>

<sup>†</sup> Joint BSC-CRG-IRB Research Program in Computational Biology, Barcelona Supercomputing Center, Jordi Girona 29, E-08034 Barcelona, Spain.

<sup>§</sup> Centro de Investigaciones Biológicas, CSIC, Ramiro de Maeztu 9, E-28040 Madrid, Spain.

<sup>||</sup> Anaxomics Biotech, Balmes 89, E-08008 Barcelona, Spain

<sup>¥</sup> ICREA, Passeig Lluís Companys 23, E-08010 Barcelona, Spain.

**ABSTRACT:** Oxidation of arylamines, such as aniline, is of high industrial interest and laccases have been proposed as biocatalysts to replace harsh chemical oxidants. However, the reaction is hampered by the redox potential of the substrate at acid pH and enzyme engineering is required to improve the oxidation. In this work, instead of trying to improve the redox potential of the enzyme, we aim towards the (transient) substrate's one and propose this as a more reliable strategy. We have successfully combined a computational approach with experimental validation to rationally design an improved biocatalyst. The *in silico* protocol combines classical and quantum mechanics to deliver atomic and electronic level detail on the two main processes involved: substrate binding and electron transfer. After mutant expression and comparison to the parent type, kinetic results show that the protocol accurately predicts aniline's improved oxidation (2-fold  $k_{\text{cat}}$  increase) in the engineered variant for biocatalyzed polyaniline production.

**KEYWORDS** Laccase, aniline, PELE, QM/MM, protein engineering, PANI, arylamines

## INTRODUCTION

There is a rising interest for replacing harsh and environmentally unfriendly industrial chemical reactions by clean enzyme-based processes.<sup>1</sup> Although the practical use of proteins remotes to ancient times, the large scale usage of well characterized enzymes in textile, detergent and starch industries is the result, in most cases, of considerable advances in biotechnology.<sup>2</sup> Protein engineering based on rational design, directed evolution and/or computer simulations have shown considerable success but altering proteins remains an arduous process.<sup>3</sup>

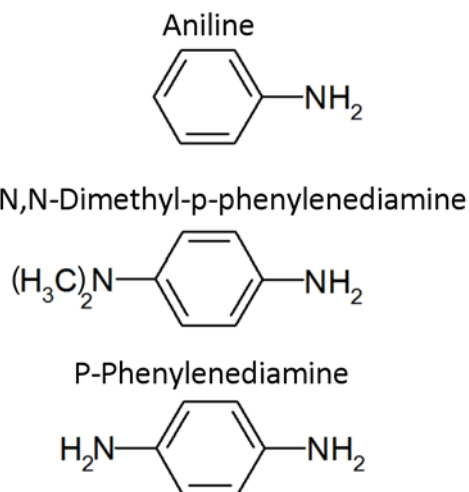
Laccases (EC 1.10.3.2) are oxidases that contain four copper ions: a tri-nuclear (T2/T3) cluster buried in the protein matrix, where molecular oxygen is reduced to water, and a T1 site, close to the surface of the protein, where substrates are oxidized. The promiscuity of these proteins toward a large number of organic compounds, use of oxygen as final electron acceptor (with no need of expensive co-factors), and production of water as sole by-product converts them into ideal biocatalysts for diverse technological purposes<sup>4</sup>. The relatively low redox potential ( $E^\circ$  0.4 - 0.8 V), when compared to other oxidoreductases such as peroxidases, limits their application<sup>5</sup> but the use of mediators has been found to expand their action toward more difficult substrates.<sup>6</sup> Trying to improve laccase's redox potential is a current strategy for increasing the oxidation capability of these proteins,<sup>7</sup> but the observation that  $K_M$  and  $k_{\text{cat}}$  of different laccases are ligand dependent evidences that oxidation is not reliant merely on the redox potential difference.<sup>7a, 7c</sup>

To advance in this matter we have used a recently developed computational protocol<sup>8</sup> that combines the protein energy landscape exploration (PELE)<sup>9</sup> software with quantum mechanics/molecular mechanics (QM/MM)<sup>10</sup> techniques. PELE is an all-atom Monte Carlo based algorithm routinely used in our labs to map long time scale dynamical processes such as global protein-substrate exploration or local induced fit events.<sup>11</sup> In redox processes, for example, we use it to identify important parameters such as donor-acceptor distance (DAD)<sup>12</sup> and the solvent accessible surface area (SASA) of the substrate.<sup>12a, 13</sup> Changes in these two parameters are expected to correlate with key variables in electron transfer theory: i) a shorter DAD points to a larger electronic coupling; ii) a smaller SASA suggests smaller solvent reorganization energy.<sup>12</sup> Then, using QM/MM we calculate spin densities on selected structures obtaining an estimation of electron transfer driving force.<sup>10a, 14</sup> In our previous study<sup>8</sup> we found that 2,6-dimethoxyphenol's enhanced oxidation by an evolved laccase was the result of substrate's rearrangement in the active site, with no important change in the redox potential of the T1 copper. In this study we challenge this computational protocol by rationally engineering a laccase for aniline (ANL) oxidation under preferred conditions for industrial application.

Aniline and its derivatives have been traditionally used in the dyestuff industry, as precursors of aniline dyes and azo dyes for textiles, hair, leather or printing,<sup>15</sup> and also as components for engineering polymers, composites and rubbers. In particular, the synthesis of conductive polyaniline (PANI) has been widely investigated during the last two decades due to its wide range of applications (sensor devices, rechargeable batteries,

etc.<sup>16</sup>). Conducting PANI macromolecules have regular head-to-tail linked monomers (over 95%) but high conductive polymer is only produced in strongly acidic conditions (pH<2.5) using oxidants such as ammonium peroxydisulfate.<sup>17</sup> To replace these processes by enzymatic bioconversion is thus a main goal,<sup>18</sup> however, aniline ( $pK_a=4.6$ ) is mostly protonated at low pH. Since the anilinium cation ( $E^\circ=1.05$  V) is much less oxidizable than non-protonated aniline (ANL) ( $E^\circ=0.63$  V), it becomes clear why laccases normally cannot oxidize this compound or reactions occur too slowly.<sup>19</sup> The high potential barrier for oxidizing aniline in acid medium<sup>20</sup> demands the use of high-redox potential laccases ( $E^\circ \sim +0.8$  V) such as the one used in this study, whereas other fungal laccases with lower redox potential, are unable to catalyze the reaction.

The strategy, presented in this work, for improving the activity of a high redox potential recombinant laccase previously obtained by directed evolution,<sup>21</sup> aims at precision enzyme design instead of screening a large number of candidates.<sup>22</sup> By means of our computational protocol, two point mutations were predicted and experimentally validated in one single protein variant. The double mutant (DM) was produced in *S. cerevisiae* and compared with the parental laccase. Kinetic analysis showed a 2-fold  $k_{cat}$  increase for ANL oxidation. Furthermore, oxidation of p-phenylenediamine (PPD), 2,2'-azino-bis(3-ethylbenzothiazoline-6-sulfonic acid) (ABTS) and N,N-dimethyl-p-phenylenediamine (DMPD – see Scheme 1 for chemical structures) was also improved 1.4, 2.0 and 1.6-fold, respectively. DMPD, in particular, is a precursor of the high-value reagent methylene blue, with applications in wide a range of fields (including as a potential antimalarial agent),<sup>23</sup> which nowadays is produced by oxidation of DMPD with ferric chloride (a highly toxic compound) with hydrogen sulfide dissolved in hydrochloric acid.



**Scheme 1. Chemical structure of all studied arylamines: aniline (ANL), n,n-dimethyl-p-phenylenediamine (DMPD) and p-phenylenediamine (PPD).**

Overall, we demonstrate the laccase's enhancement towards the above-mentioned noteworthy technological applications, re-enforcing the potential for synergetic experimental and computational protocols in predictive studies.<sup>24</sup>

## RESULTS AND DISCUSSION

The work is presented in three sections. We begin by confirming the importance of the ligand binding event<sup>8, 25</sup> in ANL oxidation by a laccase developed in a previous directed evolution experiment.<sup>21</sup> After obtaining these molecular details we rationally designed the protein binding site for improved ANL oxidation. Secondly, the precision designed variant was experimentally obtained and compared against the parent type for oxidation of ANL, DMPD and PPD, thermostability and pH range. Finally, computational cross-validation for the observed improvement DMPD's oxidation was performed.

**In silico study and rational design for ANL oxidation.** The computational protocol employed, described in the Methods section, begins by determining the binding event. For this, PELE, a Monte Carlo based molecular simulation software was employed. The program performs random substrate and protein perturbations aiming at reproducing fully flexible protein-substrate binding, including induced-fit effects. Here 120 independent 48h trajectories were produced to investigate the interactions between the laccase variants and each of the studied substrates. By analyzing the laccase-substrate interaction energy profiles produced by PELE (Figure 1) we were capable of identifying the lowest energy minima and thus the main binding modes at the T1 copper site. Once these were identified QM/MM calculations were performed to estimate the fraction of the spin density localized on the substrate. QM/MM calculations split the system into two regions: quantum and classical. In the first, which includes the T1 copper with its first coordination sphere, electronic based methods were used to study the electron transfer. The second region, the classical one, includes the rest of the system, which provides the correct geometric and electrostatic environment to the quantum region. For these calculations, 50 complexes were randomly selected using a distance and interaction energy threshold. Selection was restrained to substrates' positions within 10 Å of the T1 copper atom site and 5 kcal/mol range from the lowest interaction energy. Interaction energy plots for ANL diffusion in the parent type laccase are shown in Figure 1A.

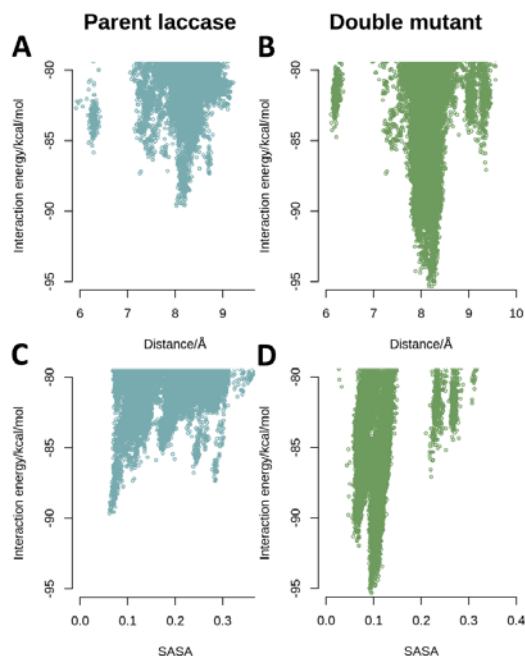


**Figure 1.** Protein-substrate interaction energies vs. distance between the center of mass of ANL and the copper T1 atom (top) and vs. SASA (bottom) for parent laccase (A, C) and double mutant (B,D).

**Table 1. Average spin densities (SP) and experimental kinetic data for parent laccase and double mutant (DM) oxidizing ANL, PPD, ABTS and DMDP .**

System	SP (%)	$k_{cat}$ ( $s^{-1}$ )	$K_M$ (mM)
Lac+ANL	12 ± 1	10.1 ± 1.1	28 ± 7.2
DM+ANL	26 ± 5	22.6 ± 3.4	59.3 ± 15.5
Lac+DMPD	39 ± 7	459 ± 18	1.7 ± 0.2
DM+DMPD	68 ± 14	741 ± 48	1.2 ± 0.2
Lac+PPD	32 ± 5	14.7 ± 0.6	3.7 ± 0.3
DM+PPD	46 ± 14	20.8 ± 2.1	3.5 ± 0.8
Lac + ABTS	23 ± 14	291 ± 18	0.0042 ± 0.001
DM + ABTS	40 ± 7	570 ± 26	0.01 ± 0.001

Observation of the lowest interacting energy complexes in the parent type protein (Figure 1A) show ANL placed in the T1 cavity close to N207, N263, S264, and H-bonded to D205 (Figure 2A). QM/MM calculations performed on randomly selected structures (see Methods section) show that these exhibit 12 % spin density (Table 1 - average over 50 snapshots).

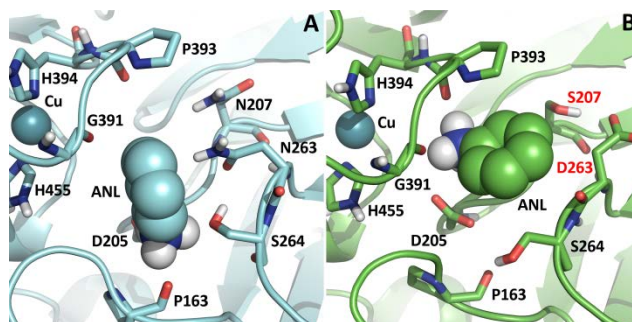


**Figure 2.** Representative minima for ANL interaction with: A) parent laccase and B) double mutant.

The next step was to re-design the binding site to improve ANL's oxidation rate (at pH 3) by this laccase. Since changing the redox potential of the copper site is a complex task, in particular in a high redox potential laccase,<sup>26</sup> and conscious of the impact of the binding event in the overall oxidation rate,<sup>7c, 8, 25b, 27</sup> we have instead targeted to locally modify ANL's (anilinium cation) redox potential. We wish to stabilize the oxidized form of ANL boosting electron transfer to the Cu T1 site which, in theory, can be accomplished by introducing a second negatively charged residue (in addition to D205) next to ANL's binding site. To test this hypothesis, we probed alternative single-point mutations. Initially, we tested mutations in position 205 since the lowest energy structures showed a direct interaction between ANL and that residue in the parent type laccase. Furthermore, literature<sup>28</sup> pointed to a potential benefit from D205E mutation but computational QM/MM scoring indicated poorer activity. Other mutations, D205Y and D205A led to similar results (all computed spin densities are available in SI). In addition to D205, two other residues are seen in direct contact with the substrate: residues 207 and 263, both asparagines. Since our criteria for selecting the mutations was to improve the electrostatic environment around the substrate we started by testing single-point mutations to aspartic acid (identical side-chain length as asparagine) on each residue (N207D/N263D). This double mutant showed considerable spin density improvement (32 %) but two aspartic acids so close each to other could be troublesome for protein stability. For this reason, we tested which of these positions would have the most beneficial effect on ANL oxidation (Table S1) and found N263D to be the best candidate. Finally, position 207 was mutated to serine because this mutation was found to be a good compromise between ligand binding, activity and protein stability. Ligand binding on the double mutant N207S/N263D (DM) displays an interaction energy profile slightly improved from the parent protein (Figure 1B), with a shorter DAD, in particular the amine group is in average closer to the Cu atom (Figure 2B), and similar SASA (Figures 1C, D)). Activity was scored with QM/MM calculations, which showed an enhanced 26 % spin density, compared with 12 % for the parent type laccase reaction (Table 1). Finally, the likelihood of disrupting protein stability was assessed through sequence analysis (see below).

Introduction of N207S/N263D modifies the substrate-protein interactions as seen in Figures 1B and 2B. The new minima show that the substrate is now located with a different orientation and the amine group closer to the copper atom thanks to the smaller side chain of S207 (Figure 2B), and enclosed be-

tween the two negatively charged D205 and D263. The presence of these two residues so close to each other could also alter their protonation states (especially at pH 3) so to verify this possibility we have used H++ server to assess the  $pK_a$  of these amino acids in the mutant protein. Predictions indicate a clear deprotonated state for both residues. Furthermore, DM interacts with ANL through the backbone carbonyl atoms of residues G391 and P393, the latter connected to the copper coordinated H394.

We have also performed a sequence space search to check if other proteins carry the proposed mutations. We found, using HotSpot Wizard (loschmidt.chemi.muni.cz /hotspotwizard), that position N207 contains 34 out of 50 times an asparagine while 5 other sequences have serines in that position (default settings used). In the case of N263 also 34 out of 50 sequences have an asparagine but only two have a glutamic and one an aspartic acid. We have further verified these results by performing a BLAST search using the Prime module of Maestro software. After multiple sequence alignment with ClustalW (in SI) we found that out of 28 sequences (with available crystal structures) one contains the substitutions proposed in the DM (Figure 3). This multicopper oxidase (MCO), sharing 29 % sequence identity with our parent type, is not a laccase but the membrane Fet3 protein from *S. cerevisiae*, which catalyzes the oxidation of Fe(II) to Fe(III) (PDB entry 1ZPU).<sup>29</sup>

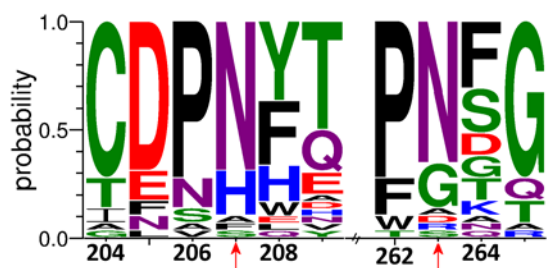


**Figure 3** – Sequence logo including the residues mutated in this work. The positions 207 and 263 are identified by a red arrow. The sequences belong to multicopper oxidases with at least 30% sequence identity to the parent type used in this work.

The fact that we find the N263S mutation in 5 other sequences and the two N207D/N263S mutations in another MCO, helps determine the probability of obtaining a stable variant.

#### Experimental validation

In order to verify the effect of the mutations predicted *in silico*, the N207S/N263D mutations were introduced in the parent laccase. The resulting DM was produced in *S. cerevisiae*, purified to 100% homogeneity and its activity with ANL at pH 3 compared with the pure parent type's (Table 1). The enzyme's turnover for aniline increased 2-fold respecting the parental laccase. Also, DM showed 1.6- and 1.4-fold improvement of  $k_{cat}$  with the aniline analogues DMPD and PPD and no increment in  $K_M$ , resulting in an enhancement of the catalytic efficiency as regards the parent type. The notably higher turnover rates of both enzymes on DMPD (respecting ANL) can be explained by the fact that, assuming that for each DMPD molecule only one nitrogen is positively charged, the reciprocal 1-4 position of the amine groups stabilizes the radical more than in ANL (since an electron donating group is para with respect to the double positive charge).

It has been shown that a conserved acid residue (D206 in *Trametes versicolor* laccase; Glu235 in *Myceliophthora albotomyces* laccase) has a key role in the oxidation of phenols by fungal laccases. This residue assists the transfer of the proton while the electron is transferred through one His coordinating T1 copper (H458 in *T. versicolor* laccase), giving rise to the phenoxy radical. The concerted electron-proton transfer firstly described by Galli and co-workers<sup>30</sup> was confirmed in a recent work<sup>27c</sup>. Nevertheless, improved oxidation of ABTS (Table 1), which does not require a proton transfer, in the mutated variants favors the idea that changes observed in  $k_{cat}$  are most likely due to an improved local oxidation of the substrate (thanks to an additional negatively charged residue) and not in a facilitated proton transfer. To validate this hypothesis we have further performed quantum calculations on a model system; the energy difference between the oxidized and non-oxidized forms of ANL in the presence and absence of a negatively charged carboxylic acid (in the same position of D263) was calculated (Table S2).<sup>31</sup> Results indicate that the energy difference, and therefore oxidation, is more favorable when the negative charge is added, corroborating our hypothesis (for further details please see SI).

The correlation between  $k_{cat}$  and spin density (%) values for both laccases (and identical results seen in other studies<sup>8, 27c</sup>), confirmed the usefulness of simulation studies for the rational design of these enzymes.

To better assess the possible benefit of this kinetic improvement for laccase application, we compared the activity and stability of the DM with the parent laccase at the working conditions for the enzymatic synthesis of polyaniline, which is pH 3 in the presence of anionic surfactants. DM presented a similar pH activity profile than the parental laccase (Figure 4A). As for the stability at acid pH, DM maintained the high stability of the parent laccase at pH 3, retaining 100 % initial activity after 5 h of incubation (Figure 4B). We also checked the laccase's thermostability since, very frequently, mutations with beneficial effects on enzyme activity might be detrimental for its stability. In this case,  $T_{50}$  (the temperature at which the activity is 50 % of the initial activity) was lowered marginally by 1.5 °C upon mutation of laccase ( $T_{50} = 63.5$  °C for DM versus  $T_{50} = 65$  °C for the parental laccase). Finally, we assayed both laccases as biocatalysts for the synthesis of water-soluble polyaniline (PANI). The enzymatic polymerization of aniline was carried out in citrate-phosphate buffer pH 3, using dodecyl-benzenesulfonate (SDBS) as doping template to provide the *p*-coupling of the protonated ANL monomers. The synthesis of PANI was followed by monitoring the increment of absorbance at 800 nm. This absorbance band is the distinctive signal for emeraldine salt that is the green, protonated and conductive form of PANI.<sup>32</sup> When DM catalyzed the reaction, the absorbance at 800 nm was significantly raised. Up to 36 % higher absorbance was obtained after 22 h of reaction with DM respecting the value obtained with the parental laccase (Figure 4C). This increment correlated with superior production of green color during the polymerization of ANL catalyzed by DM (Figure 4D).

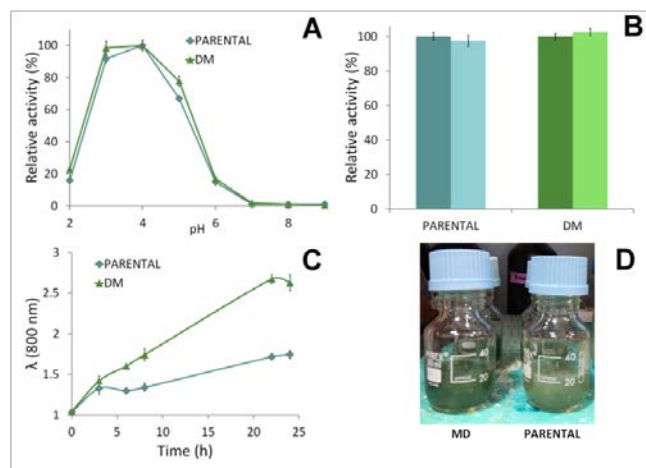


**Figure 4.** Comparison of double mutant (DM) and parental laccase for A) Optimum pH for aniline oxidation (300 mM). B) Laccase stability at pH 3 (initial activity, dark color, and residual activity after 5 h of incubation, light color, are shown). C) Enzymatic polymerization of 15 mM aniline along time (with 5 mM SDBS as template) as shown by the increase of absorbance at 800 nm. D) Green PANI produced in C by parental and DM laccases.

#### DMPD *in silico* cross-validation

The aniline derivative, DMPD, was also chosen to compare the activity of DM and parent laccase. Since kinetic analysis showed a significant  $k_{cat}$  and  $K_M$  improvement and a literature survey reveals this compound to be a precursor for the production of methylene blue, a high-value reagent, we have cross-validated the computational method with DMPD. The same protocol described for ANL was used for DMPD (keeping in mind that at pH 3 two possible protonation states can co-exist). PELE simulations for the parent type laccase and DM evidence the positive effect of both single point mutations in DAD (as conformations closer to the copper atom are possible, Figures S1, S2). N263D mutation allows DMPD to adopt a new position more favorable for the oxidation (Figure 5, results for the protonated tertiary amine where changes in DM are more pronounced). DMPD is initially interacting with H455 and A161 (Figure 5A) while in DM, it is more buried. DMPD in DM is interacting with the two acid side chains (D205 and D263) which generate a more favorable electrostatic environment for electron abstraction (Figure 5B).

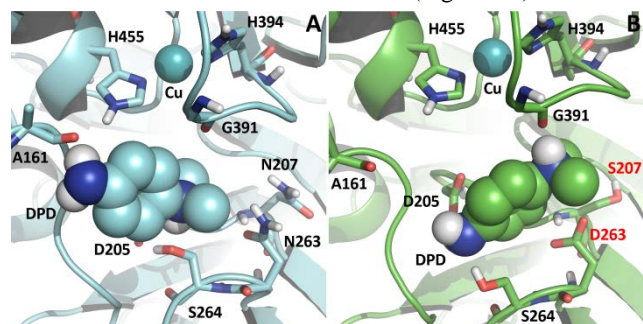


**Figure 5.** Representative minima for DMPD (protonated tertiary amine) interaction with: A) parent laccase and B) DM.

The presence of N207S/N263D mutations in the engineered laccase also displays an increased spin density of 68 % (op-

posed to 39 % for the parent laccase, Table 1) confirming that the computational method is consistently capable of reproducing the observed increase in  $k_{cat}$  for both laccase substrates. It should be noted that spin densities must be taken as relative quantities, that is to say, a reference must always be available, preferentially the parent protein. Depending on the nature of the substrate and the local environment spin densities vary greatly but in relative terms are accurate predictors for improved  $k_{cat}$ .

#### CONCLUSIONS

Based on a computational strategy optimizing DAD, SASA and protein ligand recognition, we rationally introduced two active site point mutations in a high redox potential laccase, aiming at a more favorable oxidation of ANL. Following this (classical force field) conformational space search, improved oxidation was confirmed with mixed QM/MM techniques. This combined effort provides a reliable *in silico* screening, reducing experimental validation to precisely designed mutants. In particular, the introduction of a negatively charged residue (N263D) has increased ANL's local oxidation (stabilizing the anilinium cation) and thus favoring electron transfer. Experimental results confirm that the recalcitrant oxidation of ANL shows a change in  $k_{cat}$  from 10 to 23  $s^{-1}$ . The increment of  $K_M$  is not troublesome in terms of direct industrial application since high substrate concentrations are employed. Screening for improved oxidation of DMPD evidenced the enhancement of the catalytic efficiency thanks to a simultaneous improvement of  $k_{cat}$  and  $K_M$ . For these particular cases, the computational method appears to provide not only a qualitative prediction to  $k_{cat}$  enhancement but also a notable quantitatively agreement with the computationally estimated spin density (2.2- and 1.6-fold for ANL and DMPD, respectively). Moreover, in line with earlier findings<sup>8, 25a, 33</sup> on the importance of the binding event, our results confirm that targeting the substrate's local (transient) oxidation is a reliable strategy for laccase activity improvement. These results are encouraging for future synergic computational and experimental studies aiming at bio-based oxidation of small arylamines with vast applications.

#### METHODOLOGY

**Systems setup.** The high redox potential laccase from basidiomycete PM1 (PDB entry 5ANH, provided by Dr. Javier Medrano) was used as template (96% sequence identity) for the evolved laccase.<sup>21</sup> For clarity purposes, the protein redox potentials referred along the text, unless otherwise mentioned, refer to the copper T1 site. The protein structure was prepared with assistance of Protein Preparation Wizard<sup>34</sup>, PROPKA<sup>35</sup> and the H++ web server<sup>36</sup> to determine the protonation state of all ionizable amino acids at pH 3.

Four substrates have been employed in the computational study: ANL, and DMPD, PPD and ABTS. Substrates were fully optimized with the density functional M06<sup>37</sup> with the 6-31G\*\* basis set in an implicit solvent and the electrostatic potential charges computed at the same level of theory were used in the following force field based PELE simulations. ANL was modeled as anilinium cation since it is the dominant

ing form at low pH needed for PANI production while DMPD (also studied at pH 3) was considered in two possible protonation states: charged on the primary or the tertiary amine.

**Protein-substrate binding modes.** To determine the different binding modes of substrates in the T1 copper site, PELE<sup>9a, 38</sup> simulations were performed following the protocol, described in detail in Monza *et al.*<sup>8</sup>. Since the ligand's binding site in laccases is well known, each substrate was manually placed close to the entrance of the copper site and was then free to move in a region 20 Å within the T1 copper atom. Local conformational exploration was accomplished by perturbing the ligand and the protein in a sequence of steps followed by side-chain re-adjustment (using rotamer libraries) and all-atom minimization. It should be noted that this procedure is unlike most docking approaches since, not only the dynamics of the ligand are taken into consideration, but also the protein's side chains and backbone. The new protein-substrate conformations are then accepted or rejected through a Metropolis test based on energy (E) differences computed using an OPLS force field<sup>39</sup> and a surface-generalized Born (SGB) implicit continuum solvent.<sup>40</sup> Interaction energies have been computed as  $IE = E_{PS}^{SGB} - (E_P^{SGB} + E_S^{SGB})$  where PS refers to the protein (P) substrate (S) complex. From the local laccase-substrate sampling several important parameters (that may affect electron transfer) can be extracted. In first place, by analyzing the overall interaction energy profile, we identify the best binding poses. The average DAD is also computed since changes in electronic coupling can be qualitatively estimated through this quantity.<sup>12</sup> Then, the SASA gives indications on changes on the electronic reorganization energy (its solvent component) as a more exposed ligand will have a higher energetic penalty.<sup>12a, 13, 41</sup>

**QM/MM electron transfer.** After selecting the lowest interaction energy complexes obtained in the PELE simulations these were used to estimate the amount of spin density transferred from the substrate to the copper T1 site. For this, we have used QM/MM methods which employ both quantum mechanics and molecular mechanics.<sup>10, 14</sup> QSite<sup>42</sup> was used, including in the quantum region the entire copper site (with equatorial and axial ligands) as well as the substrate. The M06-L<sup>43</sup> density functional with lacvp\* basis set was used (LANL2DZ effective core basis set for the copper atom and 6-31G\* for the rest of the atoms). The remaining part of the protein was modeled in the molecular mechanics section through an all-atom OPLS force field. Mulliken<sup>44</sup> populations were computed to characterize the spin density transferred from the substrate to the copper site. Previous studies have shown that these are insensitive to the functional employed and initial guess used for the wavefunction (specifying localized spin on either the donor/acceptor or neither at the beginning of the calculation does not change the results).<sup>8</sup> Also, previous experimental and theoretical studies have shown that spin density correlates well with oxidation potentials of donors in ET proteins, establishing if an unpaired electron is energetically more stable on the donor or acceptor's molecular orbitals.<sup>8, 45</sup>

The rationale behind the choice of the point mutations presented in this work consists in increasing spin density along with decreasing SASA and DAD which is expected to lead to an improvement in  $k_{cat}$ .<sup>8</sup> Aiming to simultaneously reduce the

solvent reorganization energy and improve the driving force is justified by the high reorganization energy of laccases (above 30 kcal/mol<sup>7c</sup>), which safely places our designs far from Marcus inverted region.<sup>13</sup> Otherwise, more attention should be paid on the driving force-reorganization energy balance.

**Reagents and enzymes.** DMPD, ANL and the *S. cerevisiae* transformation kit were purchased from Sigma-Aldrich. The high pure plasmid isolation kit was purchased from Roche. Zymoprep yeast plasmid miniprep II kit was purchased from Zymo Research and the plasmid midi kit and QIAquick gel extraction kit from QIAGEN. Pfu Ultra High-Fidelity DNA polymerase was purchased from Agilent Technologies.

**Strains and culture media.** The uracil-independent and ampicillin-resistance shuttle pJRoc30 vector carrying the parent laccase construct under the control of the GAL1 promoter was generated as previously described.<sup>46</sup> The protease deficient *S. cerevisiae* BJ5465 strain was grown in YPD medium. Minimal expression medium contained 100 mL 67g/L sterile yeast nitrogen base, 100 ml 19.2 g/L sterile yeast synthetic dropout medium supplement without uracil, 100 mL sterile galactose 20%, 67 mL KH<sub>2</sub>PO<sub>4</sub> 1M pH 6.0 buffer, 1 mL sterile CuSO<sub>4</sub> 1M, 1 mL sterile chloramphenicol 25 mg/mL in ethanol and 631 mL (ddH<sub>2</sub>O).

**Site directed mutagenesis/IVOE.** Mutations N207S and N263D were introduced in the laccase sequence by *in vivo* overlap extension (IVOE).<sup>47</sup> Four mutagenic primers were designed to obtain overlapping ends: N207SFW (5'-TGCGACCGTCTTACACG-3'), N207SRV (5'-CGTGTAAGACGGGTCGCA-3'), N263DFW (5'-CCTTCCCCGACTCCGGGACCA-3') and N263DRV (5'-TGGTCCCCGAGTCGGGAAGG-3'). Also, we used primer RMLN sense (5'-CCTCTATACTTTAACGTCAAGG-3') which binds to nucleotides 160–180 of the plasmid; and primer RMLC antisense (5'-GGGAGGGCGTGAATGTAAGC-3'), which binds to nucleotides 2031–2050 of the plasmid. The 5'-end gene fragment was amplified with RMLN and reverse mutagenic N207SRV primer, the center fragment with N207SFW and N263DRV primers, and the 3'-end fragment with RMLC and forward mutagenic N263DFW primer.

All polymerase chain reactions (PCR) mixtures were prepared in a final volume of 50µL containing 0.25 µM of each primer, 1µM of dNTPs, 2.5 U *Pfu* ultra DNA polymerase and 100 ng of pJRalac<sup>21</sup> was used as template. Reactions were performed as follows: 95 °C for 2 min (1 cycle) 94 °C for 0.5 min, 55 °C for 0.5 min and 74 °C for 2 min (28 cycles); and 72 °C for 10 min (1 cycle).

Purified PCR products were co-transformed in yeast together with the linearized expression vector. Transformed cells were plated in SC dropout plates<sup>46a</sup> and incubated for 2 days at 28 °C.

**Laccase production and purification.** Laccase was produced in 1-L flask cultures, in minimal expression medium, at 30 °C, 200 rpm. Crude extracts were separated by centrifugation at 12000 rpm at 4 °C, then, filtered using a 0.45 µm pore size membrane and concentrated by ultra-filtration through 10000 MWCO membranes and dialyzed against 20 mM Tris-HCl buffer, pH 7. Laccases were purified by HPLC (AKTA purifier, GE Healthcare) in two anion-exchange and one molecular exclusion steps: first, using a HiPrep Q FF 16/10 column and a

100 mL gradient of 0 – 40 % elution buffer (20 mM Tris-HCl + 1 M NaCl, pH 7); second, using a Mono Q HR 5/5 column and a 30 mL gradient of 0 – 25 % elution buffer; and finally using a HiLoad 16/600 Superdex 75 pg column and 20 mM Tris-HCl + 150 mM NaCl, pH 7 (all columns from GE Healthcare). Fractions containing laccase activity were pooled, dialyzed and concentrated between each chromatographic step.

**Laccase characterization. Kinetic constants.** Substrate oxidation was measured by the increment of absorbance at 550 nm for DMPD ( $\epsilon_{550} = 4134 \text{ M}^{-1}\text{cm}^{-1}$ ) and 410 nm for aniline ( $\epsilon_{410} = 1167 \text{ M}^{-1}\text{cm}^{-1}$ ) using the plate reader Spectramax Plus (Molecular Devices). Reactions were carried out in triplicate, in 50 mM citrate-phosphate buffer pH 3.0, in 250  $\mu\text{L}$  final volume. Initial rates were represented versus substrate concentration and fitted to a single rectangular hyperbola function in SigmaPlot (version 10.0) software, where parameter  $a$  was equal to  $k_{cat}$  and parameter  $b$  was equal to  $K_M$ .

**Optimum pH.** Plates containing 10  $\mu\text{L}$  of laccase samples with 0.1 U/mL activity (measured with 3 mM 2,2'-azino-bis(3-ethylbenzothiazoline-6-sulfonic acid), ( $\epsilon_{418} = 36000 \text{ M}^{-1}\text{cm}^{-1}$ ) and 180  $\mu\text{L}$  of 100 mM Britton and Robinson buffer were prepared at pH values of 2, 3, 4, 5, 6, 7 and 8. The assay commenced when 10  $\mu\text{L}$  of 60 mM ABTS was added to each well to give a final substrate concentration of 3 mM. Activities were measured in triplicate in kinetic mode and the relative activity was calculated as a percentage of the maximum activity of each variant in the assay.

**Stability at pH 3.** 40  $\mu\text{L}$  laccase with 0.1 U/mL activity (measured as aforementioned), were added to 150  $\mu\text{L}$  citrate-phosphate buffer 50 mM, pH 3. Plates were incubated for 5 hours at room temperature. The residual activity was measured in triplicate in kinetic mode in the plate reader, and the relative activity was calculated as a percentage of the initial activity. One activity unit was defined as the amount of enzyme needed to transform 1  $\mu\text{mol}$  ABTS/minute.

**Thermostability.**  $T_{50}$  was evaluated as previously described<sup>21</sup>

**Enzymatic polymerization of aniline.** Oxidation of 15 mM aniline was carried out in 25 mL 50 mM Citrate-phosphate pH 3, using 5 mM sodium dodecylbenzenesulfonate (SDBS) as template. The reaction was performed with 0.1 U/mL laccase activity (measured with 3 mM DMPD pH 3) of crude enzyme, in Pyrex bottles maintaining a 1:1 medium: air ratio (v/v), at room temperature, for 24 h in constant stirring. Increase in 800 nm absorbance was followed in triplicate.

## ASSOCIATED CONTENT

**Supporting Information.** This material is available free of charge via the Internet at <http://pubs.acs.org>.

Average spin densities for unsuccessful mutations, PELE interaction energy profiles for DMPD, Protein sequence alignment for multi-copper proteins with available crystal structures

## AUTHOR INFORMATION

### Corresponding Author

\* victor.guallar@bsc.es

\* susanacam@cib.csic.es

### Author Contributions

‡These authors contributed equally.

## Funding Sources

This study was supported by the INDOX (KBBE-2013-7-613549) EU-project, and the NOESIS (BI0201456388-R) and OxiDesign (CTQ2013-48287-R) Spanish project. GS thanks an FPI grant of the Spanish Ministry of Competitiveness.

## Notes

The authors have no conflict of interest to declare.

## ABBREVIATIONS

ABTS, 2,2'-azino-bis(3-ethylbenzothiazoline-6-sulfonic acid); ANL, aniline; DAD, donor-acceptor distance; DM, double mutant; DMPD, N,N-dimethyl-p-phenylenediamine; PANI, polyaniline; PELE, protein energy landscape exploration; PPD, p-phenylenediamine; QM/MM, quantum mechanics/molecular mechanics; SASA, solvent accessible surface area; SDBS, sodium dodecyl-benzenesulfonate.

## REFERENCES

1. Waites, M. J.; Morgan, N. L.; Rockey, J. S.; Higton, G., *Industrial Microbiology: An Introduction*. Wiley: 2001.
2. Kirk, O.; Borchert, T. V.; Fuglsang, C. C., Industrial enzyme applications. *Curr. Opin. Biotechnol.* **2002**, *13*, 345-351.
3. (a) Kiss, G.; Çelebi-Ölçüm, N.; Moretti, R.; Baker, D.; Houk, K. N., Computational Enzyme Design. *Angew. Chem., Int. Ed.*, *52*, 5700-5725; (b) Kries, H.; Blomberg, R.; Hilvert, D., De novo enzymes by computational design. *Curr. Opin. Chem. Biol.* **2013**, *17*, 221-228; (c) Hilvert, D., Design of Protein Catalysts. *Annu. Rev. Biochem.* **2013**, *82*, 447-470; (d) Ye, L. J.; Toh, H. H.; Yang, Y.; Adams, J. P.; Snajdrova, R.; Li, Z., Engineering of Amine Dehydrogenase for Asymmetric Reductive Amination of Ketone by Evolving Rhodococcus Phenylalanine Dehydrogenase. *ACS Catal.* **2015**, *5*, 1119-1122; (e) Verges, A.; Cambon, E.; Barbe, S.; Salamone, S.; Le Guen, Y.; Moulis, C.; Mulard, L. A.; Remaud-Siméon, M.; André, I., Computer-Aided Engineering of a Transglycosylase for the Glucosylation of an Unnatural Disaccharide of Relevance for Bacterial Antigen Synthesis. *ACS Catal.* **2015**, *5*, 1186-1198; (f) Mellot-Draznieks, C.; Valayannopoulos, V.; Chrétien, D.; Munnich, A.; de Lonlay, P.; Toulhoat, H., Relative Enzymatic Activity Levels from In Silico Mutagenesis. *ACS Catal.* **2012**, *2*, 2673-2686; (g) Bloom, J. D.; Arnold, F. H., In the light of directed evolution: Pathways of adaptive protein evolution. *Proc. Natl. Acad. Sci. U. S. A.* **2009**, *106*, 9995-10000.
4. (a) Mayer, A. M.; Staples, R. C., Laccase: new functions for an old enzyme. *Phytochemistry* **2002**, *60*, 551-565; (b) Minussi, R. C.; Pastore, G. M.; Durán, N., Potential applications of laccase in the food industry. *Trends Food Sci. Technol.* **2002**, *13*, 205-216; (c) Osma, J. F.; Toca-Herrera, J. L.; Rodríguez-Couto, S., Uses of Laccases in the Food Industry. *Enzyme Res.* **2010**, *2010*, 918761; (d) Riva, S., Laccases: blue enzymes for Green Chem.. *Trends Biotechnol.* **2006**, *24*, 219-226; (e) Cañas, A. I.; Camarero, S., Laccases and their natural mediators: Biotechnological tools for sustainable eco-friendly processes. *Biotechnol. Adv.* **2010**, *28*, 694-705; (f) Witayakran, S.; Ragauskas, A. J., Synthetic

Applications of Laccase in Green Chem.. *Adv. Synth. Catal.* **2009**, *351*, 1187-1209.

5. (a) Martínez, Á., High Redox Potential Peroxidases. In *Industrial Enzymes*, Polaina, J.; MacCabe, A., Eds. Springer Netherlands: 2007; pp 477-488; (b) Ayala, M., Redox Potential of Peroxidases. In *Biocatalysis Based on Heme Peroxidases*, Torres, E.; Ayala, M., Eds. Springer Berlin Heidelberg: 2010; pp 61-77.

6. (a) Bourbonnais, R.; Paice, M. G., Oxidation of non-phenolic substrates. *FEBS Letters* **1990**, *267*, 99-102; (b) Camarero, S.; Ibarra, D.; Martínez, Á. T.; Romero, J.; Gutiérrez, A.; del Río, J. C., Paper pulp delignification using laccase and natural mediators. *Enzyme Microb. Technol.* **2007**, *40*, 1264-1271.

7. (a) Li, K.; Xu, F.; Eriksson, K.-E. L., Comparison of Fungal Laccases and Redox Mediators in Oxidation of a Nonphenolic Lignin Model Compound. *Appl. Environ. Microbiol.* **1999**, *65*, 2654-2660; (b) Morozova, O. V.; Shumakovich, G. P.; Shleev, S. V.; Yaropolov, Y. I., Laccase-mediator systems and their applications: A review. *Appl. Biochem. Microbiol.* **2007**, *43*, 523-535; (c) Tadesse, M. A.; D'Annibale, A.; Galli, C.; Gentili, P.; Sergi, F., An assessment of the relative contributions of redox and steric issues to laccase specificity towards putative substrates. *Org. Biomol. Chem.* **2008**, *6*, 868-878; (d) Xu, F., Oxidation of Phenols, Anilines, and Benzenethiols by Fungal Laccases: Correlation between Activity and Redox Potentials as Well as Halide Inhibition†. *Biochemistry* **1996**, *35*, 7608-7614; (e) Xu, F.; Kuly, J. J.; Duke, K.; Li, K.; Krikstopaitis, K.; Deussen, H.-J. W.; Abbate, E.; Galinyte, V.; Schneider, P., *Appl. Environ. Microbiol.* **2000**, *66*, 2052-2056.

8. Monza, E.; Lucas, M. F.; Camarero, S.; Alejaldre, L. C.; Martínez, A. T.; Guallar, V., Insights into Laccase Engineering from Molecular Simulations: Toward a Binding-Focused Strategy. *J. Phys. Chem. Lett.* **2015**, *6*, 1447-1453.

9. (a) Borrelli, K. W.; Vitalis, A.; Alcántara, R.; Guallar, V., PELE: Protein Energy Landscape Exploration. A Novel Monte Carlo Based Technique. *J. Chem. Theo. Comp.* **2005**, *1*, 1304; (b) Cossins, B. P.; Hosseini, A.; Guallar, V., Exploration of Protein Conformational Change with PELE and Meta-Dynamics. *J. Chem. Theory Comput.* **2012**, *8*, 959-965.

10. (a) Friesner, R. A.; Guallar, V., Ab Initio Quantum Chemical and Mixed Quantum Mechanics/Molecular Mechanics (QM/MM) Methods for Studying Enzymatic Catalysis. *Annu. Rev. Phys. Chem.* **2005**, *56*, 389-427; (b) Gao, J.; Truhlar, D. G., Quantum mechanical methods for enzyme kinetics. *Annu. Rev. Phys. Chem.* **2002**, *53*, 467-505.

11. (a) Babot, E. D.; del Río, J. C.; Cañellas, M.; Sancho, F.; Lucas, F.; Guallar, V.; Kalum, L.; Lund, H.; Gröbe, G.; Scheibner, K.; Ullrich, R.; Hofrichter, M.; Martínez, A. T.; Gutiérrez, A., Steroid hydroxylation by basidiomycete peroxxygenases: A combined experimental and computational study. *Appl. Environ. Microbiol.* **2015**, *81*, 4130-4142; (b) Lucas, M.F.; Guallar, V., An Atomistic View on Human Hemoglobin Carbon Monoxide Migration Processes. *Biophys. J.* **2012**, *102*, 887-896; (c) Linde, D.; Pogni, R.; Cañellas, M.; Lucas, F.; Guallar, V.; Baratto, Maria C.; Sinicropi, A.; Sáez-Jiménez, V.; Coscolín, C.; Romero, A.; Medrano, Francisco J.; Ruiz-Dueñas, Francisco J.; Martínez, Angel T., Catalytic surface radical in dye-decolorizing peroxidase: a computational, spectroscopic and site-directed mutagenesis

study. *Biochem. J* **2015**, *466*, 253-262; (d) Hosseini, A.; Espóna-Fiedler, M.; Soto-Cerrato, V.; Quesada, R.; Pérez-Tomás, R.; Guallar, V., Molecular Interactions of Prodiginines with the BH3 Domain of Anti-Apoptotic Bcl-2 Family Members. *PLoS ONE* **2013**, *8*, e57562.

12. (a) Winkler, J. R.; Gray, H. B., Electron Flow through Metalloproteins. *Chem. Rev* **2014**, *114*, 3369-3380; (b) Christensen, N. J.; Kepp, K. P., Setting the stage for electron transfer: Molecular basis of ABTS-binding to four laccases from *Trametes versicolor* at variable pH and protein oxidation state. *J. Mol. Catal. B: Enzym.* **2014**, *100*, 68-77.

13. Marcus, R. A., Electron transfer reactions in chemistry. Theory and experiment. *Rev. Mod. Phys.* **1993**, *65*, 599-610.

14. Senn, H.; Thiel, W., QM/MM Methods for Biological Systems. In *Atomistic Approaches in Modern Biology*, Reiher, M., Ed. Springer Berlin Heidelberg: 2007; Vol. 268, pp 173-290.

15. Morris, P.; Travis, A., History of the International Dyestuff Industry. *Am. Dyest. Rep.* **1992**, *81*, 59-59.

16. (a) Bhadra, S.; Khastgir, D.; Singha, N. K.; Lee, J. H., Progress in preparation, processing and applications of polyaniline. *Prog. Polym. Sci.* **2009**, *34*, 783-810; (b) Ćirić-Marjanović, G., Recent advances in polyaniline research: Polymerization mechanisms, structural aspects, properties and applications. *Synth. Met.* **2013**, *177*, 1-47.

17. Sapurina, I. Y.; Stejskal, J., Oxidation of aniline with strong and weak oxidants. *Russ. J. Gen. Chem.* **2012**, *82*, 256-275.

18. (a) Kobayashi, S.; Makino, A., Enzymatic Polymer Synthesis: An Opportunity for Green Polymer Chemistry. *Chem. Rev* **2009**, *109*, 5288-5353; (b) Hollmann, F.; Arends, I. W. C. E.; Buehler, K.; Schallmeyer, A.; Buhler, B., Enzyme-mediated oxidations for the chemist. *Green Chem.* **2011**, *13*, 226-265; (c) Gross, R. A.; Kumar, A.; Kalra, B., Polymer Synthesis by In Vitro Enzyme Catalysis. *Chem. Rev* **2001**, *101*, 2097-2124; (d) Bornscheuer, U. T.; Huisman, G. W.; Kazlauskas, R. J.; Lutz, S.; Moore, J. C.; Robins, K., Engineering the third wave of biocatalysis. *Nature* **2012**, *485*, 185-194.

19. Zhang, J.; Zou, F.; Yu, X.; Huang, X.; Qu, Y., Ionic liquid improves the laccase-catalyzed synthesis of water-soluble conducting polyaniline. *Colloid Polym. Sci.* **2014**, *292*, 2549-2554.

20. Yang, L. Y. O.; Chang, C.; Liu, S.; Wu, C.; Yau, S. L., Direct Visualization of an Aniline Admolecule and Its Electropolymerization on Au(111) with in Situ Scanning Tunneling Microscope. *J. Am. Chem. Soc.* **2007**, *129*, 8076-8077.

21. Pardo, I.; Vicente, A. I.; Mate, D. M.; Alcalde, M.; Camarero, S., Development of chimeric laccases by directed evolution. *Biotechnol. Bioeng.* **2012**, *109*, 2978-2986.

22. (a) Privett, H. K.; Kiss, G.; Lee, T. M.; Blomberg, R.; Chica, R. A.; Thomas, L. M.; Hilvert, D.; Houk, K. N.; Mayo, S. L., Iterative approach to computational enzyme design. *Proc. Natl. Acad. Sci. U. S. A.* **2012**, *109*, 3790-3795; (b) Frushicheva, M. P.; Cao, J.; Chu, Z. T.; Warshel, A., Exploring challenges in rational enzyme design by simulating the catalysis in artificial kemp eliminase. *Proc. Natl. Acad. Sci. U. S. A.* **2010**, *107*, 16869-16874; (c) Chen, C.-Y.; Georgiev, I.; Anderson, A. C.; Donald, B. R., Computational structure-



- based redesign of enzyme activity. *Proc. Natl. Acad. Sci. U. S. A.* **2009**, *106*, 3764-3769.
23. (a) Nematollahi, D.; Maleki, A., Electrochemical oxidation of N,N-dialkyl-p-phenylenediamines in the presence of arylsulfonic acids. An efficient method for the synthesis of new sulfonamide derivatives. *Electrochem. Commun.* **2009**, *11*, 488-491; (b) Meissner, P.; Mandi, G.; Coulibaly, B.; Witte, S.; Tapsoba, T.; Mansmann, U.; Rengelshausen, J.; Schiek, W.; Jahn, A.; Walter-Sack, I.; Mikus, G.; Burhenne, J.; Riedel, K.-D.; Schirmer, R. H.; Kouyate, B.; Muller, O., Methylene blue for malaria in Africa: results from a dose-finding study in combination with chloroquine. *Malar. J.* **2006**, *5*, 84; (c) Schirmer, R. H.; Coulibaly, B.; Stich, A.; Scheiwein, M.; Merkle, H.; Eubel, J.; Becker, K.; Becher, H.; Müller, O.; Zich, T.; Schiek, W.; Kouyaté, B., Methylene blue as an antimalarial agent. *Redox Rep.* **2003**, *8*, 272-275; (d) Coulibaly, B.; Zoungrana, A.; Mockenhaupt, F. P.; Schirmer, R. H.; Klose, C.; Mansmann, U.; Meissner, P. E.; Müller, O., Strong Gametocytocidal Effect of Methylene Blue-Based Combination Therapy against Falciparum Malaria: A Randomised Controlled Trial. *PLoS ONE* **2009**, *4*, e5318.
24. (a) Karplus, M.; Lavery, R., Significance of Molecular Dynamics Simulations for Life Sciences. *Isr. J. Chem.* **2014**, n/a-n/a; (b) Lucas, Maria F.; Cabeza de Vaca, I.; Takahashi, R.; Rubio-Martínez, J.; Guallar, V., Atomic Level Rendering of DNA-Drug Encounter. *Biophys. J.* **2014**, *106*, 421-429.
25. (a) Pardo, I.; Santiago, G.; Gentili, P.; Lucas, F.; Monza, E.; Medrano, F. J.; Galli, C.; Martínez Ferrer, A. T.; Guallar, V.; Camarero, S., RE-DESIGNING THE SUBSTRATE BINDING POCKET OF LACCASE FOR ENHANCED OXIDATION OF SINAPIC ACID. *Catal.: Sci. Technol* **2015**; (b) Toscano, M. D.; De Maria, L.; Lobedanz, S.; Østergaard, L. H., Optimization of a Small Laccase by Active-Site Redesign. *ChemBioChem* **2013**, *14*, 1209-1211.
26. (a) Xu, F.; Berka, R. M.; Wahleithner, J. A.; Nelson, B. A.; Shuster, J. R.; Brown, S. H.; Palmer, A. E.; Solomon, E. I., Site-directed mutations in fungal laccase: effect on redox potential, activity and pH profile. *Biochem. J* **1998**, *334*, 63-70; (b) Xu, F.; Palmer, A. E.; Yaver, D. S.; Berka, R. M.; Gambetta, G. A.; Brown, S. H.; Solomon, E. I., Targeted Mutations in a *Trametes villosa* Laccase: axial perturbations of the T1 copper. *J. Biol. Chem.* **1999**, *274*, 12372-12375; (c) Cambria, M. T.; Gullotto, D.; Garavaglia, S.; Cambria, A., In silico study of structural determinants modulating the redox potential of *Rigidoporus lignosus* and other fungal laccases. *J. Biomol. Struct. Dyn.* **2012**, *30*, 89-101.
27. (a) Koschorreck, K.; Richter, S. M.; Swierczek, A.; Beifuss, U.; Schmid, R. D.; Urlacher, V. B., Comparative characterization of four laccases from *Trametes versicolor* concerning phenolic C-C coupling and oxidation of PAHs. *Arch. Biochem. Biophys.* **2008**, *474*, 213-219; (b) Galli, C.; Gentili, P.; Jolivalt, C.; Madzak, C.; Vadalà, R., How is the reactivity of laccase affected by single-point mutations? Engineering laccase for improved activity towards sterically demanding substrates. *Appl. Microbiol. Biotechnol.* **2011**, *91*, 123-131; (c) Pardo, I.; Santiago, G.; Gentili, P.; Lucas, F.; Monza, E.; Medrano, F. J.; Galli, C.; Martínez, A. T.; Guallar, V.; Camarero, S., Re-designing the substrate binding pocket of laccase for enhanced oxidation of sinapic acid. *Catal.: Sci. Technol* **2016**, *474*.
28. Madzak, C.; Mimmi, M. C.; Caminade, E.; Brault, A.; Baumberger, S.; Briozzo, P.; Mougin, C.; Jolivalt, C., Shifting the optimal pH of activity for a laccase from the fungus *Trametes versicolor* by structure-based mutagenesis. *Protein Eng., Des. Sel.* **2006**, *19*, 77-84.
29. Taylor, A. B.; Stoj, C. S.; Ziegler, L.; Kosman, D.; Hart, P. J., The copper-iron connection in biology: structure of the metallo-oxidase Fet3p. *Proc. Natl. Acad. Sci. U. S. A.* **2005**, *102*, 15459-15464.
30. Galli, C.; Madzak, C.; Vadalà, R.; Jolivalt, C.; Gentili, P., Concerted Electron/Proton Transfer Mechanism in the Oxidation of Phenols by Laccase. *ChemBioChem* **2013**, *14*, 2500-2505.
31. Méndez-Hernández, D. D.; Tarakeshwar, P.; Gust, D.; Moore, T. A.; Moore, A. L.; Mujica, V., Simple and accurate correlation of experimental redox potentials and DFT-calculated HOMO/LUMO energies of polycyclic aromatic hydrocarbons. *J. Mol. Model.* **2013**, *19*, 2845-2848.
32. Junker, K.; Gitsov, I.; Quade, N.; Walde, P., Preparation of aqueous polyaniline-vesicle suspensions with class III peroxidases. Comparison between horseradish peroxidase isoenzyme C and soybean peroxidase. *Chem. Pap.* **2013**, *67*, 1028-1047.
33. Toscano, M. D.; De Maria, L.; Lobedanz, S.; Østergaard, L. H., Optimization of a Small Laccase by Active-Site Redesign. *ChemBioChem* **2013**, *14*, 1209-1211.
34. Sastry, G.; Adzhigirey, M.; Day, T.; Annabhimoju, R.; Sherman, W., Protein and ligand preparation: parameters, protocols, and influence on virtual screening enrichments. *J. Comput. Aid. Mol. Des.* **2013**, *27*, 221-234.
35. Olsson, M.; Sondergaard, C.; Roskowski, M.; Jensen, J., PROPKA3: Consistent Treatment of Internal and Surface Residues in Empirical pKa Predictions. *J. Chem. Theory Comput.* **2011**, *7*, 525-537.
36. Anandakrishnan, R.; Aguilar, B.; Onufriev, A. V., H++ 3.0: automating pK prediction and the preparation of biomolecular structures for atomistic molecular modeling and simulations. *Nucleic Acids Res.* **2012**, *40*, W537-W541.
37. Zhao, Y.; Truhlar, D., The M06 suite of density functionals for main group thermochemistry, thermochemical kinetics, noncovalent interactions, excited states, and transition elements: two new functionals and systematic testing of four M06-class functionals and 12 other functionals. *Theor. Chem. Acc.* **2008**, *120*, 215-241.
38. Madadkar-Sobhani, A.; Guallar, V., PELE web server: atomistic study of biomolecular systems at your fingertips. *Nucleic Acids Res.* **2013**, *41*, W322-W328.
39. Kaminski, G. A.; Friesner, R. A.; Tirado-Rives, J.; Jorgensen, W. L., Evaluation and Reparametrization of the OPLS-AA Force Field for Proteins via Comparison with Accurate Quantum Chemical Calculations on Peptides†. *The J. Phys. Chem. B* **2001**, *105*, 6474-6487.
40. Bashford, D.; Case, D. A., Generalized Born models of macromolecular solvation effects. *Annu. Rev. Phys. Chem.* **2000**, *51*, 129-152.
41. Bortolotti, C. A.; Siwko, M. E.; Castellini, E.; Ranieri, A.; Sola, M.; Corni, S., The Reorganization Energy in Cytochrome c is Controlled by the Accessibility of the Heme to the Solvent. *J. Phys. Chem. Lett.* **2011**, *2*, 1761-1765.
42. Murphy, R.; Philipp, D.; Friesner, R., A mixed quantum mechanics/molecular mechanics (QM/MM) method

for large-scale modeling of chemistry in protein environments. *J. Comp. Chem.* **2000**, *21*, 1442-1457.

43. Zhao, Y.; Truhlar, D. G., Density Functionals with Broad Applicability in Chemistry. *Acc. Chem. Res.* **2008**, *41*, 157-167.

44. Mulliken, R. S., Electronic Population Analysis on LCAO-MO Molecular Wave Functions. I. *The J. Chem. Phys.* **1955**, *23*, 1833-1840.

45. (a) Artz, K.; Williams, J. C.; Allen, J. P.; Lenzian, F.; Rautter, J.; Lubitz, W., Relationship between the oxidation potential and electron spin density of the primary electron donor in reaction centers from *Rhodobacter sphaeroides*. *Proc. Natl. Acad. Sci. U. S. A. of the United States of America* **1997**, *94*, 13582-13587; (b) Meisel, D.; Neta, P., One-electron redox potentials of nitro compounds and radiosensitizers. Correlation

with spin densities of their radical anions. *J. Am. Chem. Soc.* **1975**, *97*, 5198-5203.

46. (a) Camarero, S.; Pardo, I.; Cañas, A. I.; Molina, P.; Record, E.; Martínez, A. T.; Martínez, M. J.; Alcalde, M., Engineering Platforms for Directed Evolution of Laccase from *Pycnoporus cinnabarinus*. *Appl. Environ. Microbiol.* **2012**, *78*, 1370-1384; (b) Maté, D.; García-Burgos, C.; García-Ruiz, E.; Ballesteros, A. O.; Camarero, S.; Alcalde, M., Laboratory Evolution of High-Redox Potential Laccases. *Chem. Biol.* **2010**, *17*, 1030-1041.

47. Alcalde, M., Mutagenesis Protocols in *Saccharomyces cerevisiae* by In Vivo Overlap Extension. In *In Vitro Mutagenesis Protocols*, Braman, J., Ed. Humana Press: 2010; Vol. 634, pp 3-14.

SYNOPSIS TOC Improved aniline oxidation by computational protein engineering

---

